JOURNAL OF MECHANICAL ENGINEERING AND SCIENCES (JMES)
ISSN: 2289-4659 e-ISSN: 2231-8380
VOL. 15, ISSUE 1, 7715 – 7728
DOI: https://doi.org/10.15282/jmes.15.1.2021.08.0608

ORIGINAL ARTICLE

Optimization of ultimate tensile strength of welded Inconel 625 and duplex 2205

S. Madhankumar[1,*], K. Manonmani[2], V. Karthickeyan[3,4], N. Balaji[3]

[1] Department of Mechatronics Engineering, Sri Krishna College of Engineering and Technology, Coimbatore, India, 641008
Phone: +91 8344483282; Fax: 0422-2678012
[2] Department of Mechanical Engineering, Alagappa Chettiar Government College of Engineering and Technology, Karaikudi, India, 630004
[3] Deparment of Mechanical Engineering, Sri Krishna College of Engineering and Technology, Coimbatore, India, 641008
[4] Department of Chemical Engineering, National Cheng Kung University, No. 1, University Road, Tainan 70101, Taiwan

ABSTRACT – The ultimate strength is an important property of any material for the manufacturing of components. This paper utilized the laser beam welding (LBW), due to its smaller dimension, which produces lesser distortion and process velocity is higher. Inconel 625 alloy and duplex 2205 stainless steel is having higher strength and corrosive resistance properties. Due to the above-mentioned properties, it could be used in oil and gas storage containers, marine and geothermal applications. This research work presents an investigation of various input variable effects on the output variable (ultimate tensile strength) in LBW for dissimilar materials namely, Inconel 625 alloy and duplex 2205 stainless steel. The input variables for this research are the power of a laser, welding speed, and focal position. The experimental runs are developed with the help of design of experiment (DOE) and utilized statistical design expert software. The ultimate tensile strength on different runs is measured using a universal tensile testing machine. Then from a response surface methodology and ANOVA, the optimum value of ultimate tensile strength was determined to maximize the weld joint and bead geometry. Finally, the confirmation test was carried out, it reveals the maximum error of 0.912% with the predicted value. In addition, the microstructure of the weld beads was examined using optical microscopy.

ARTICLE HISTORY
Received: 26th Dec 2019
Revised: 16th July 2020
Accepted: 01st Aug 2020

KEYWORDS
Laser beam welding;
Inconel 625 alloy;
duplex 2205;
ultimate tensile strength;
microstructure

INTRODUCTION

Welding is a process of fitting together the surfaces of two metals over localized meld. It is a cost-effective, precise and reliable for joining two metals it may similar or dissimilar metals. None of the practice is as broadly used to join efficiently. The laser beam is used to weld metals of multiple pieces by LBW. This laser beam gives a rigorous source of heat, deep weld joint and slim. The welding speed is proportionate to the supplied power and it's also related to the thickness and type of the workpiece [1]. Pulsed Nd: YAG laser welding is a neodymium-doped yttrium aluminium garnet (Nd: YAG) a laser is a solid-state laser, Nd: YAG laser operating in both pulsed and continuous mode. The Nd: YAG laser makes laser light usually close to an infrared region of the spectrum at 1064 nm. The Nd: YAG laser is a commonly used type of solid-state laser in many fields at present because of its good thermal properties and easy repairing. The pulsed Nd: YAG laser welding system contains a laser, beam delivery and, focusing head.

The advantages Nd: YAG laser welding is very small heat-influencing zone due to a very short pulse duration (welding time, 5-10 ms) and a relatively slow sequence of the individual welding pulses (up to 10Hz). One of the main advantages of laser welding is its versatility. Another important fact is that laser systems can be made fully automatic in order to have high accuracy welds. Improvements in welding speed, productivity and accuracy are achieved at the same time. Very high finish welds are obtained, that do not require further processing. These qualities make lasers a good choice for welding a variety of parts like transmission components, antilock-brake valves; pace-makers, and stainless-steel tubes. Lasers provide a high heat concentration that is obtained when the beam is focused to a metal surface, resulting in deep, narrow welds with a minimum of melted metal, which reduces undesirable effects such as distortion and large heat-affected zones (HAZs). The high welding speeds and low scrap rates achieved with the laser process make it cost-effective for stainless steel applications.

Earlier work by Costa AP et al. [2] concluded that horizontal and vertical focal point positions were important parameters to avoid overheating and to achieve high resistant joints respectively and also the continuous Nd: YAG laser was originated to give the best results. Aimed at achieving the maximum ultimate tensile strength by making the usage of Nd: YAG laser for thin plate magnesium alloy welding process parameters such as shielding gas, conveying the speed of workpiece, laser energy, pulse shape, and pulse frequency were optimized using the Taguchi analytical methodology. As the output of research, the optimal combination of welding parameters for laser welding is Ar as the shielding gas, a 360W laser, a workpiece speed of 25mm/s, a pulse frequency of 160Hz, a laser focus distance of 0.2mm and a type III pulse shape. The maximum stress was found in the 23rd welding zone at the overlap of approximately 75%. The optimal result was inveterate with a maximum tensile stress of 169MPa, two and a half times greater than that from the original set for laser welding [3]. Benyounis et al. [4] optimized the keyhole parameters of carbon steel in counter-clockwise CO_2

*CORRESPONDING AUTHOR | S. Madhankumar | ✉ madhankumars@skcet.ac.in

laser welding (butt) of medium carbon steel in design-expert software. The optimum weld bead was found between the welding power (1.2kW - 1.24kW), welding sped (69.77cm/min - 70cm/min) and focused position (-2.03mm to - 1.71mm). El-Batahgy [5] focused on optimizing the gas flow as well as the protection of gas device design. The study found the protection against oxidation is easiest with helium than with more dense gases (such as nitrogen or argon), better surface state for the molten zone, less perturbed by the mechanical effect of the gas. Also, the high ionization potential of helium is an important element in the case of CO_2 laser welding, because it permits the best efficiency for the laser-matter interaction. In the case of Nd: YAG laser, where plasma is very difficult to initiate, it can be replaced by denser gases (such as nitrogen or argon) in order to improve the welding penetration by mechanical pressure. A nozzle system was developed to assures protection against oxidation using minimal gas flow rates and increases welding penetration [6]. Utilized the Taguchi method for experimental design [7]. The Pulsed Nd: YAG laser welding of AISI 304 to AISI 420 stainless steel plates were examined. The welds were examined for cracks, defects and for determining the weld geometry in an optical microscope. Tensile testing was underpinned to access weld strength [8]. Examined the effects of process parameters such as welding speed, laser power, pressure and laser beam size on weld seam width and lap-shear strength for laser transmission welding of acrylic sheet in lap joint configuration using a laser diode device. Increasing laser power increases lap-shear strength and weld-seam width; although increasing welding speed decreases both responses, weld seam width increases with line energy (until it reaches a maximum limit) as the stand-off distance increases [9]. Studied methodology of the response surface and study of techniques of variance from [9], [10]. For Inconel 625 alloy and stainless duplex steel SAF 2205 the ultimate strength values are 760MPa and 620MPa, respectively. From these previous works, it is clear that to optimize the laser power and welding speed are significant process parameters that can improve the efficiencies of welding.

METHODS AND MATERIALS

In this work, Butt welding of Inconel 625 and Duplex Stainless steel SAF 2205 is carried out by varying the input parameters since it's extensively used in chemical tanks & pipes, automotive, boiler & vessel manufacturing, heat exchange equipment, power plants, and reactor applications. The size of the workpiece was 30 mm wide, 30 mm long and 2 mm thickness. Inconel is a family of austenitic nickel chromium-based superalloys. Inconel alloys are corrosion resistant material well suited for service in extreme environments subjected to pressure and heat. It has a good combination of yield strength, tensile strength, creep strength, excellent processability, weldability and good resistance to high-temperature corrosion on prolonged exposure to aggressive environments. Strength of Inconel alloy 625 is derived from the stiffening effect of molybdenum and Niobium on its nickel-chromium matrix, thus precipitation hardening treatments are not required. Table 1 shows the chemical composition of Inconel 625. Characteristics of Inconel 625 are high creep-rupture strength, oxidation resistant to 1800°F, seawater pitting and crevice corrosion resistant, immune to chloride-ion stress corrosion cracking and non-magnetic [11]. Duplex 2205 stainless steel (both ferritic and austenitic) is used extensively in applications that require good corrosion resistance and strength. The S31803 grade stainless steel has undergone a number of modifications resulting in UNS S32205 and was endorsed in the year 1996. This grade offers higher resistance to corrosion. At temperatures above 300°C, the brittle micro-constituents of this grade undergo precipitation, and at temperatures below -50°C the micro-constituents undergo ductile-to-brittle transition; hence this grade of stainless steel is not suitable for use at these temperatures. Applications are oil and gas exploration, processing equipment, transport, storage and chemical processing, high chloride and marine environments, paper machines, liquor tanks, pulp, and paper digesters [12]. Table 1 gives the chemical composition of duplex stainless steel SAF 2205.

Table 1. Chemical Composition of Inconel 625 and Duplex stainless steel SAF 2205

Base	Composition (% Weight)										
	Ni	Cr	Mo	Fe	Ti	C	Mn	Si	Nb	V	W
Inconel 625	59.6	22.85	8.1	4.81	0.19	0.082	0.11	0.1	3.50	0.01	0.14
Duplex stainless steel SAF 2205	4.81	22.81	3.05	66.9	0.006	0.028	1.43	0.5	0.03	0.12	0.21

In this work, a systematic method the Design of Experiments **(**DOE) is used to evaluate the relationship between factors influencing a welding process and the output of that process [13]. To optimize output parameters, DOE is required to control process inputs. And, response surface method is used to examine the relationship between one or more response variables and a set of quantitative experimental parameters. These methods are often employed after the important controllable factors have been identified and intend to find the factor setting that optimizes the response [14]. The three-level response surface factorial design utilized in this study. The aim of the variance analysis (ANOVA) is to analyse the welding process parameters affect the quality characteristic significantly. This is accomplished by separating the total

variability of the S/N ratios, which is measured by the sum of the squared deviations from the total mean of the S/N ratio, into contributions by each welding process parameter and the error. The test for significance of the regression model, the test for significance on individual model coefficients and the lack-of-fit test were performed using Design Expert 7 software [15]. ANOVA tables summarise the analysis of three variances of the responses and show the significant models [16]. F Value: Test for comparing model variance with residual (error) variance. When the variances are close to each other, the ratio will be close to one and it is less likely that any of the factors have a significant effect on the response.

Experimental Details

The Figure 1 (a) shows the Nd-YAG Robotic Laser Beam welding equipment. The experiments are conducted on High peak power pulsed ND: YAG Laser welding system with six degrees of freedom robot delivered through 300µm luminator fiber., JK 300D, made by GSI group laser division, United Kingdom which is available with M/s. Optilase Techniks (I) PVT. LTD. Chennai, Tamilnadu. The maximum average power produced at laser is 300W, it ranges from 0W to 600W. Table 2 gives the laser beam welding parameters.

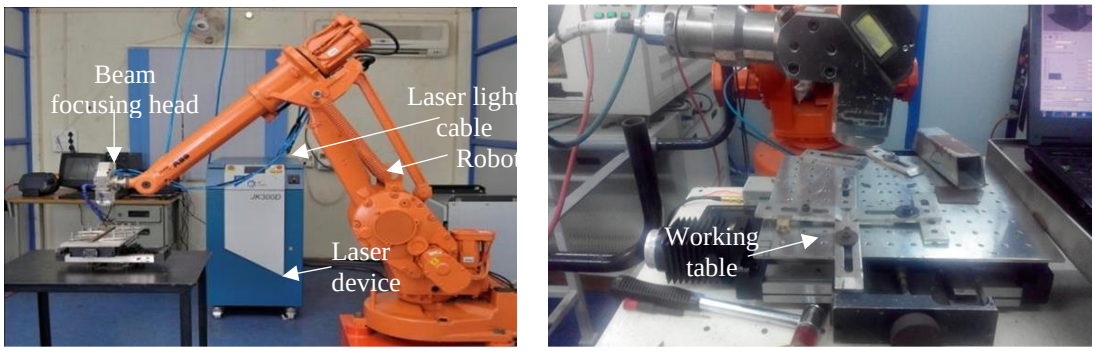

(a) (b)

Figure 1. (a) Nd: YAG Robotic Laser Beam welding equipment and (b) experimental setup of Nd: YAG laser welding

Table 2. Laser beam welding parameters

S. No	Welding Parameters	
1	Type of Laser	Pulsed Nd: YAG laser welding
2	Maximum Average power at Laser	300W
3	Type of gas used as medium	Argon
4	Work piece dimensions	30mm ×30mm× 2mm
5	Type of joint	Butt joint with no filler material
6	Location of work piece	At the center of table using specially designed fixture
7	Spot diameter	0.5mm
8	Wavelength	1064nm
9	Gas pressure	0.5bar

The laser beam is focused at the interface of the joints. No filler material is used for the laser welding of the samples. An inert gas such as argon is used to protect the weld bead from contamination, and to reduce the formation of absorbing plasma. Figure 1(b) shows an experimental Setup of Nd: YAG laser welding. The samples are cut into square specimens of 30mm x 30mm by using a wire cut electric discharge machine to avoid distortion.

Laser welding parameters for pulsed Nd: YAG laser

As shown in Table 3 three welding parameters visualizing laser beam power (LP), focal position (FP) and welding speed (WS) are considered as input parameters. So, this experiment is having 3 factors and 3 – 3 – 3 level factorial design. We know that for full factorial design the number of possible designs N equals to level power factors. Table 4 gives the 12 runs developed for pulsed Nd: YAG laser welding from DOE.

Table 3. Welding parameters for Pulsed Nd: YAG Laser welding

Notation	Parameters	Levels		
		1	2	3
LP	Laser Power (W)	400	500	600
WS	Welding Speed (mm/min)	300	450	600
FP	Focal Position (mm)	14	16	18

Table 4. DOE for Pulsed Nd: YAG Laser welding

Std	Run	Block	Factor 1 Laser Power (W)	Factor 2 Welding Speed (mm/min)	Factor 3 Focal Position (mm)
6	1	Block 1	600	450	14
12	2	Block 1	500	600	18
4	3	Block 1	600	600	16
8	4	Block 1	600	450	18
3	5	Block 1	400	600	16
10	6	Block 1	500	600	14
1	7	Block 1	400	300	16
9	8	Block 1	500	300	14
5	9	Block 1	400	450	14
2	10	Block 1	600	300	16
11	11	Block 1	500	300	18
7	12	Block 1	400	450	18

Optical Microscopy and Tensile strength test

Before going to take microstructure, the weld samples were cut into transverse directions and the cross-sectional surface was carried out for the standard metallographic procedure. Polishing with emery sheets of SiC with grit size varying from 220 to 2000 followed by disc polishing using alumina and velvet cloth were employed on the specimen to obtain a mirror finish the weldments [17]. Metallurgical characterization was performed with the use of an optical microscope and inverted microscope on the weldment, compromising of base metal and fusion zone. The standard metallographic procedure was adopted to prepare the sample for examination. The microstructure was revealed using an etchant glycergia (10% HNO_3+ 10% HCl + 5% acetic acid) and the etching time is 8-10 seconds. The weld bead microstructures are observed by using an optical microscope and image analyzer. The welded joints are sliced using power hacksaw and then machined to the required dimension to prepare a tensile specimen as shown in the figure, these specimens are taken in the normal direction of the weld. The specimen is loaded and the tensile specimen undergoes deformation. The tensile test of the butt joint was conducted by using a universal testing machine of 1000KN capacity.

RESULTS AND DISCUSSION

Based on the experiment, it was found that the process parameters such as laser power, welding speed, focal position have significant effect on weld bead geometrical features such as microstructures and tensile strength.

Microstructure Analysis

The weld bead microstructures are observed by using an optical microscope and image analyzer. Figure 2 shows the microstructures of the weldments, confirming that the microstructure of the weld zone (WZ) is fine, as a consequence of the high solidification and cooling speed, being generated by the high rate of heat extraction from the welded joint. No cracks are seen in the WZ, regardless of whether the region analyzed is close to the interface with the Inconel 625 (Base Metal 1 – BM1) and Duplex stainless steel SAF 2205 (Base Metal 2 – BM2).

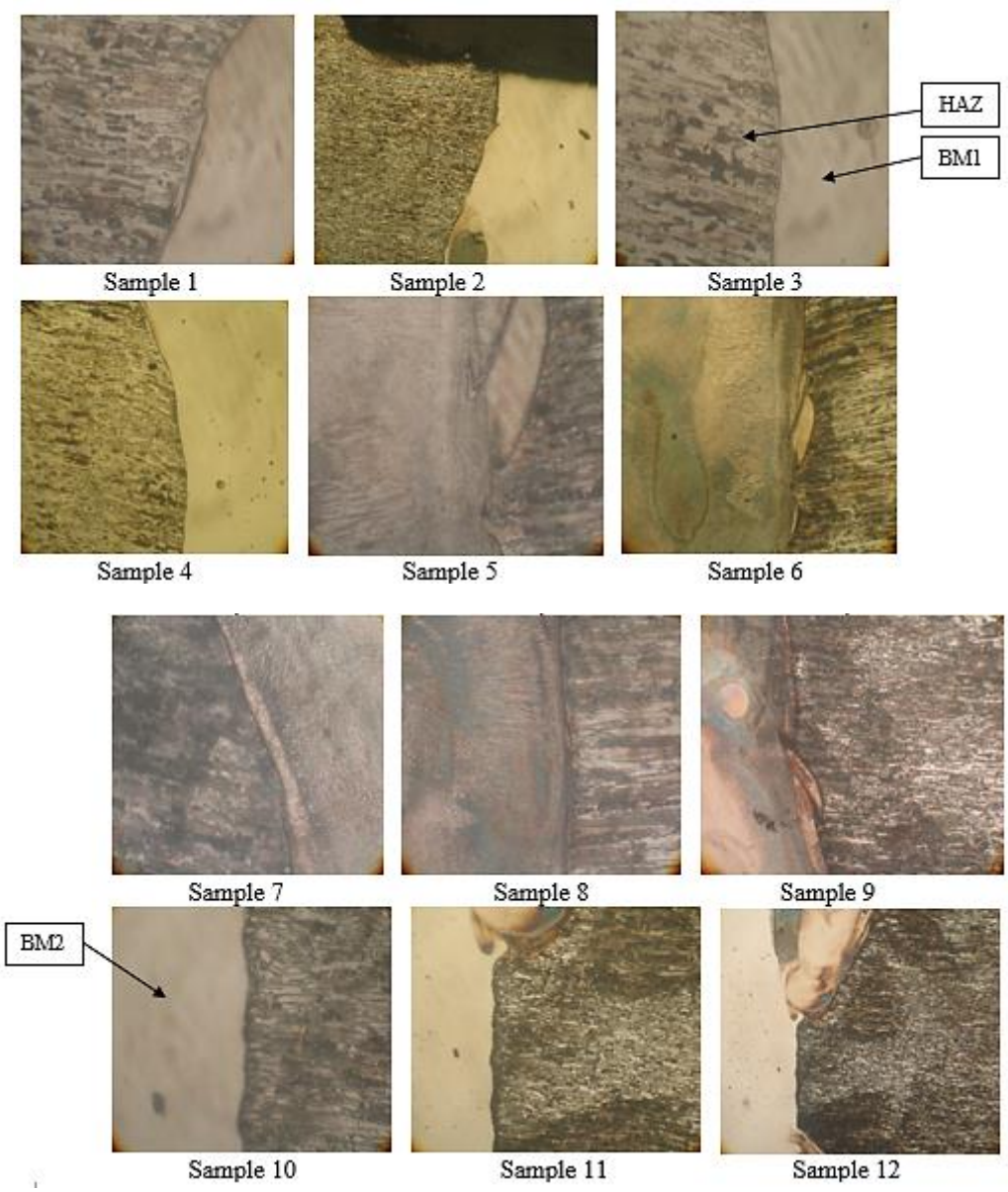

Figure 2. Microstructures of the weldments

Both columnar and fine cellular growth was observed at the fusion zone adjacent to Inconel 625 side. The fusion zone microstructure adjacent to the interface of both the metals was observed to have multi-directional grain growth containing cellular, columnar dendritic, and equiaxed grains. This could be reasoned out to the use of low welding speed which tends to reduce the cooling rate. Table 5 gives the Previous studies on welding on Dissimilar materials. On comparison with Table 5, the microstructural and tensile strength of the chosen materials gives satisfying results.

Table 5. Previous studies on welding on dissimilar materials

Ref.	Welding type	Material	Microstructural characteristics	Parameters	Maximum tensile strength
[18]	Gas tungsten arc welding process	Inconel 718 with 310 stainless steel	Optical microscope and scanning electron microscope (SEM)	Voltage, current and welding speed	495MPa
[19]	Laser beam welding	Inconel 625 with Duplex stainless steel 2205	SEM	Laser power, welding speed and energy input	~660MPa
[20]	Pulsed current gas tungsten arc welding	Inconel 718 with AISI 416	Optical microscopy, SEM	Voltage, current, frequency and Duty cycle	525MPa

Table 5. Previous studies on welding on dissimilar materials (cont.)

Ref.	Welding type	Material	Microstructural characteristics	Parameters	Maximum tensile strength
[21]	Fusion welding	316 stainless steel with Inconel 182	Optical microscopy, SEM	Fusion boundaries	-
[22]	TIG welding	22Cr15Ni3.5CuNbN steel with Inconel 617	Optical microscope	Base metal with 923 K	466.3MPa
[23]	TIG welding	AISI 316L SS with Inconel 600	Optical microscope	Diffusion coefficient, Carbon activity and carbon potential	665MPa

Tensile Test Analysis

From table 6, it is identified that the minimum ultimate tensile strength of 428MPa is obtained at 400W laser power, 600mm/min welding speed and 16mm focal position. Whereas, the maximum ultimate tensile strength of 457MPa is obtained at 500W power, 300mm/min welding speed and 14mm focal position**.** Figure 3 shows the specimens prepared for tensile testing.

Table 6. Ultimate tensile strength values

Std	Run	Block	Input Parameter			Output Parameter
			Factor 1	Factor 2	Factor 3	
			Laser Power (W)	Welding Speed (mm/min)	Focal Position mm)	Ultimate tensile strength (MPa)
6	1	Block 1	600	450	14	455
12	2	Block 1	500	600	18	433
4	3	Block 1	600	600	16	439
8	4	Block 1	600	450	18	440
3	5	Block 1	400	600	16	428
10	6	Block 1	500	600	14	441
1	7	Block 1	400	300	16	442
9	8	Block 1	500	300	14	457
5	9	Block 1	400	450	14	436
2	10	Block 1	600	300	16	456
11	11	Block 1	500	300	18	445
7	12	Block 1	400	450	18	432

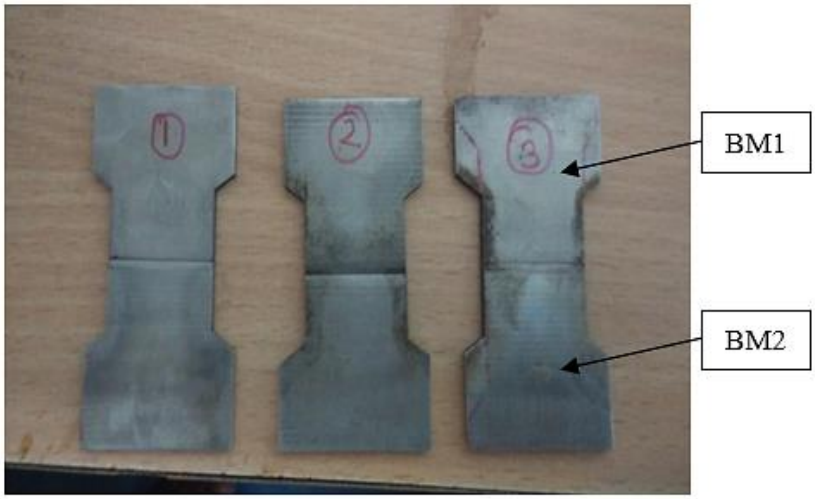

Figure 3. Tensile strength specimens

Development of mathematical models

Design-Expert statistical software is used for graphical representation of the analysis results obtained by experimental work. At this stage, the fit summary in the design-expert software is used to select the models that best describe the response factors. The fit summary includes sequential model sum squares to select the highest order polynomial where additional terms are significant and the model is not aliased. In addition, model summary statistics of the fit summary focuses on the model that maximizes adjusted R-squared and predicted R-squared values. The sequential F-test is carried out using the same statistical software package to check if the regression model is significant and find out the significant model terms of the developed models as well. The step-wise regression method is also applied to eliminate the insignificant model terms automatically.

Response model selection

Suitable response models for the response factors are selected based on the fit summaries. Design expert software is used to develop and select the model that best described the response factor in regression analysis. The sequential F test is carried out to check significance of the regression model and determine the significant model terms of the developed model as given in Table 7. Sequential model sum of squares is also included in this model to select the highest order polynomial where additional terms are significant and the model is not aliased. In addition, model summary statistics shown in Table 8 is focusing on the model that maximized adjusted R-squared and predicted R-squared values. The data of Tables 7 and 8 indicate that a quadratic model is statistically significant for the weld strength and can be used for further analysis in this investigation.

Table 7. Sequential model sum of squares for strength model

Source	Sum of Squares	df	Mean square	F Value	p-value Prob > F	
Mean vs Total	2.344E+006	1	2.344E+006			
Linear vs Mean	963.25	3	321.08	40.93	< 0.0001	Suggested
2FI vs Linear	36.50	3	12.17	2.32	0.1927	
Quadratic vs 2FI	24.50	2	12.25	21.00	0.0172	Aliased
Cubic vs Quadra	1.75	3	0.58			Aliased
Residual	0.000	0				
Total	2.345E+006	12	1.954E+005			

Table 8. Model summary statistics for strength model

Source	Std. Dev.	R-Squared	Adjusted R-Squared	Predicted R-Squared	PRESS	
Linear	2.80	0.9388	0.9159	0.8624	141.19	Suggested
2FI	2.29	0.9744	0.9437	0.8526	151.20	
Quadratic	0.76	0.9983	0.9937	0.9727	28.00	Aliased
Cubic						Aliased

Analysis of variance (ANOVA)

In factorial design technique, (ANOVA) is usually carried out to determine the significance of model and model terms. A model or model term is significant when its p-value is less than 0.05. The ANOVA for the weld strength (response) as influenced by the input variables is shown in Table 9. It is seen from Table 6 that the linear effects of laser power, welding speed and focal position also the quadratic effects of the laser power (P2), welding speed (S2) and the focal position (F2) is significant. Further, it is seen from Table 5.5 that the predicted R^2 value of 0.9983 is very close to the adj. R^2 of 0.9937. The R^2 value of 0.9727 is high and close to 1 which is an indication of an adequate model. Adequate precision compares the range of the predicted value at the design points to the average prediction error. The value of adequate precision is 44.033. The adequate precision ratio above four indicates adequate model discrimination.

Table 9. ANOVA for the model

Source	Sum of Squares	df	Mean Square	F Value	p-Value Prob > F	
Model	1024.25	8	128.03	219.48	0.0005	Significant
A-LASR POWER	338.00	11	338.00	579.43	0.0002	
B-WELDING SPEED	453.13	1	453.13	745.93	0.0001	
C-FOCAL POSITION	190.13	1	190.13	325.93	0.0004	
AB	2.25	1	2.25	3.86	0.1443	
AC	30.25	1	30.25	51.86	0.0055	
BC	4.00	1	4.00	6.86	0.0791	
A^2	15.12	1	15.12	25.93	0.0146	
B^2	0.50	1	0.50	0.86	0.4228	
C^2	0.000	0				
Residual	1.75	3	0.58			
Cor Total	1026.00	11				
Std. Dev.	0.76		R-Squared		0.9983	
Mean	442.00		Adj R-Squared		0.9937	
C.V. %	0.17		Pred R-Squared		0.9727	
PRESS	28.00		Adeq Precision		44.033	

Interaction Effect Plot using Design-Expert

Figure 4 and figure 5 shows an interaction and contour effect of welding speed and laser power on ultimate tensile strength with constant focal position 14 mm. Figure 6 and figure 7 shows an interaction effect of welding speed and focal position on ultimate tensile strength with constant laser power 500 W. Figures 4 and 5 reveal that the ultimate tensile strength increases linearly with increasing laser power and decreasing welding speed. It is apparent from figures 6 and 7 that the ultimate tensile strength increases as the focal position and the welding speed decreases. At elevated welding speed, the time accessible for the laser beam in direct contact with the surface is lower and the ultimate tensile strength increases as the welding speed decreases. The lower laser input power decreases, resulting in less hardening of the base material than the melting of the material, therefore the ultimate tensile strength decreases. Its laser power should also be held at such an optimal amount that the rise in laser power does not melt the surface but instead heat the surface.

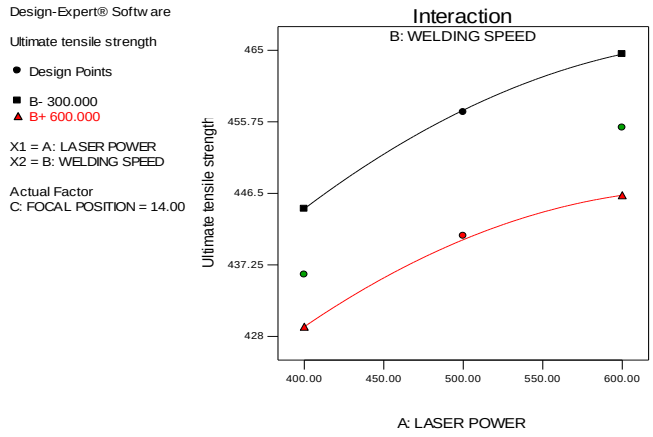

Figure 4. Interaction effect of welding speed and laser power on ultimate tensile strength with constant focal position 14mm

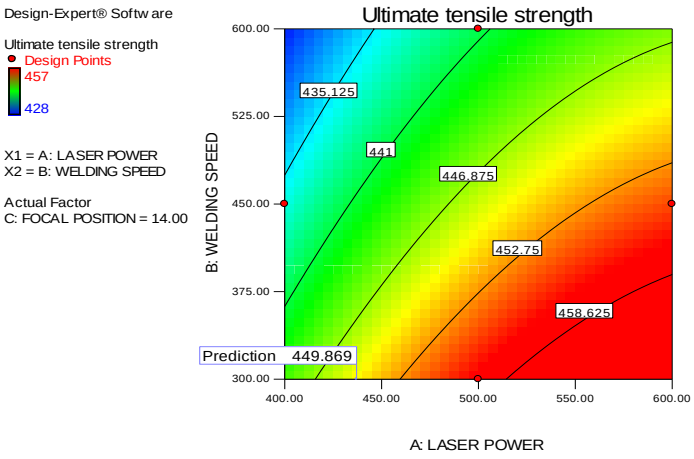

Figure 5. Contour effect of laser power and welding speed parameters on the focal position 14mm

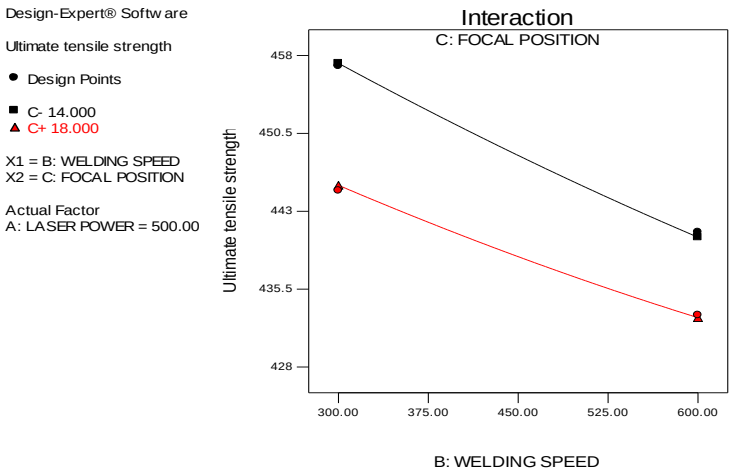

Figure 6. Interaction effect of welding speed and focal position on ultimate tensile strength with constant laser power 500W

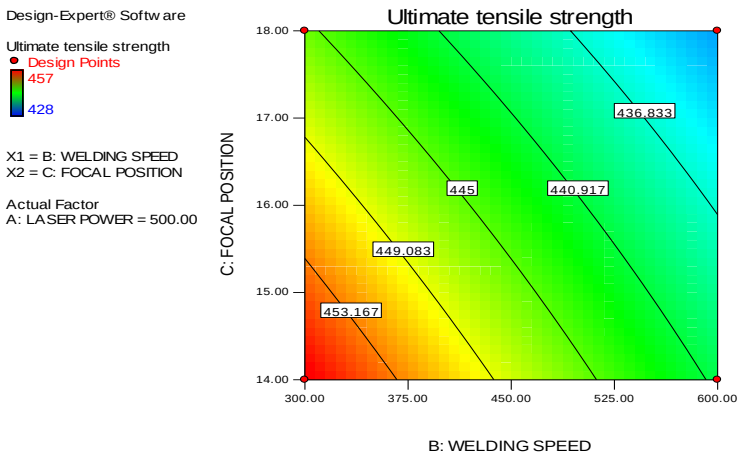

Figure 7. Contour effect of welding speed and focal position on ultimate tensile strength with constant laser power 500W

Confirmatory Test Result

Two criteria are introduced in this numerical optimization. The first set of criteria is to create a full-depth penetration weld and maximize weld penetration depth, resistance length and shearing force with no limitation on either process parameters or weld width. In this case, all the process parameters and weld width (first response) are set within a specified range. Furthermore, lowering the laser power and increasing the welding speed are the most common techniques used in automotive industries to produce relatively low-cost and excellent weld joints. Table 10 summarizes these two criteria, lower and upper limits as well as the importance of each input and response factor.

Table 10. Optimization criteria used in this study

Constraints		Lower limit	Upper limit
Name	Goal		
Laser power	Minimize	400	600
Welding speed	Minimize	300	600
Focal position	Minimize	14	18
Ultimate tensile strength	Maximize	428	457

Validation of the developed models

In order to validate the developed models, three confirmation experiments were carried out with welding conditions chosen randomly from the optimization results. For the actual responses, the average of three measured results was calculated. Table 11 summarizes the experiment's condition, the average of actual experimental values, the predicted values and the percentages of error. The validation results demonstrated that the models developed are quite accurate as the percentages of error in prediction were in a good agreement.

The normal probability plot of the residuals and plot of the residuals versus the predicted response shown in figures 8 and 9 respectively are other tools for checking the adequacy of the model. Because the points on the normal probability plot of the residuals form a straight line, it can be concluded that the model is adequate. Points in figure 8 shows no obvious pattern and unusual structure. These plots indicate the adequacy of the model.

Table 11. Validation test results

Laser power	Welding speed	Focal position	Tensile strength	
			Actual	451
437.35	300	14	Predicted	449.906
			Error %	0.501
			Actual	451.23
434.18	300	14	Predicted	449.469
			Error %	0.062
			Actual	451.71
439.75	300	14	Predicted	450.208
			Error %	0.912

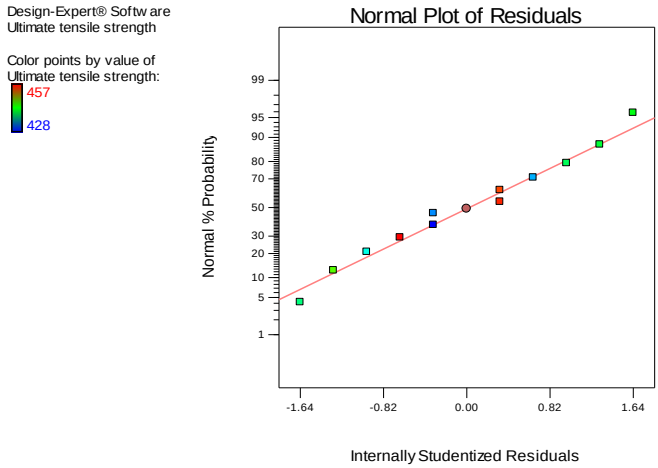

Figure 8. Normal probability plot of the residuals

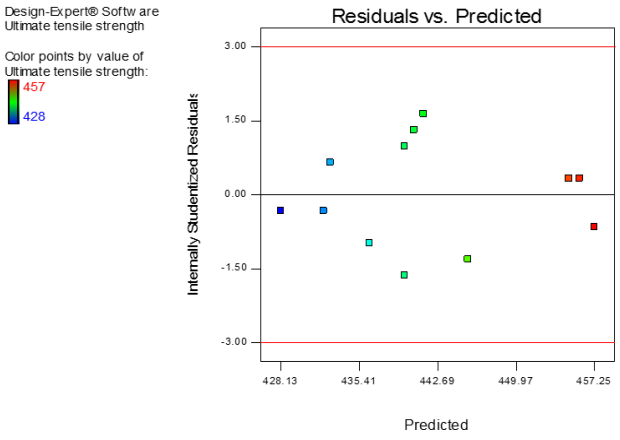

Figure 9. Plot of the residuals versus the predicted response

The validity of the proposed model can be checked by conducting three confirmation experiments. These experiments were carried out using random welding within the ranges of parameters for which the model had been derived. The small percentage of error between the actual and predicted values of the response indicates that the proposed model can predict approximately good results. Figure 10 shows the relationship between the actual and predicted values of the weld tensile

strength. This figure also indicates that the developed model is adequate and predicted results are in good agreement with the experimental data.

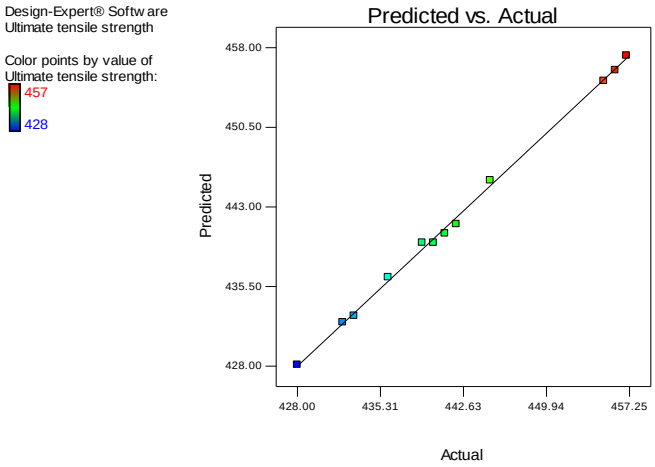

Figure 10. Plot of actual versus predicted strengths

Graphical optimization

It is obvious that the graphical optimization allows visual selection of the optimum welding conditions according to certain criteria. The result of the graphical optimization is the overlay plots, these types of plots are extremely practical for quick technical use in the workshop to choose the values of the welding parameters that would achieve certain response value for these types of materials.

In this case, for each response, the limits lower and/or upper have been chosen according to the numerical optimization results. The same two criteria, which are proposed in the numerical optimization, are introduced in the graphical optimization. As shown in Figure 11, the yellow areas on the overlay plots are the regions that meet the proposed criteria. The green/shaded areas on the overlay plots are the regions that meet the proposed criteria.

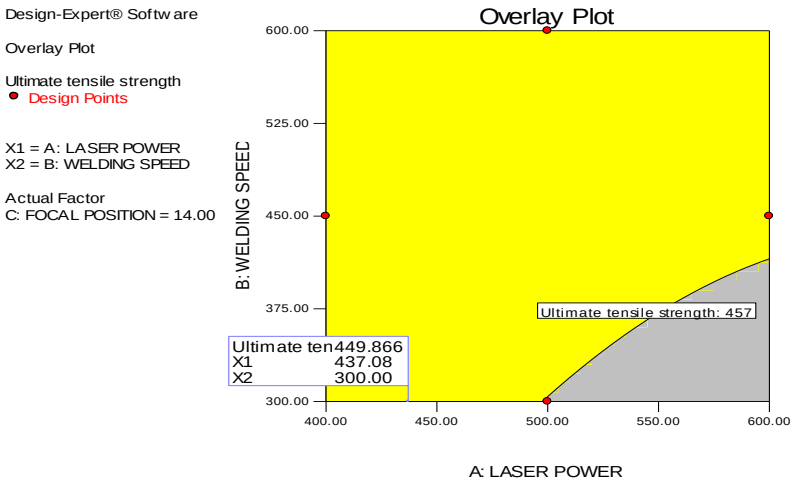

Figure 11. Overlay plot shows the region of optimal welding condition

CONCLUSIONS

This work demonstrated the porosity free successful dissimilar joints of Inconel 625 and SAF 2205 utilizing a low kW capacity Nd: YAG welding machine. The metallurgical and mechanical characterization of the weldments have been established which would be a major resource for the end-users employing these dissimilar metals. The major conclusions drawn from this work are given below:

1. The microstructure of the fusion zone exhibited multidirectional grain growth consisting of cellular, dendritic, and equiaxed grains. There is a concentration gradient of the iron and nickel elements in the WZ.

2. Tensile failures were observed at the fusion zone in all the trials. The joint strength of the laser welds is found to be 459MPa.
3. Maximum tensile strength (457MPa) was achieved for a combination of parameter namely laser power (500), travelling speed (300) and focal position (14). While minimum tensile strength (428MPa) was observed at laser power (400), travelling speed (600) and Focal position (16).
4. The ANOVA analysis also conducts to know the percentage contribution of the input parameters on output parameters. The parametric study indicates that the percentage contribution of laser power is of 35.09%, welding speed of 45.17% and focal position of 19.74% for ultimate tensile strength, which shows that the influence of focal position on ultimate tensile strength is less compare to other parameters.
5. The data obtained from laser welding of Inconel 625 and Duplex stainless steel can be used in different optimization techniques and the optimization result found in each case should be compared. The best optimization technique in which desired the result is obtained should be adopted.

ACKNOWLEDGMENTS

The authors would like to thank the Faculty of Engineering Design, Government College of Technology, Coimbatore, India and also thank Ms. P. Nandhini for technical support and guidance.

REFERENCES

[1] N. Kashaev, V. Ventzke, G. Çam, "Prospects of laser beam welding and friction stir welding processes for aluminum airframe structural applications," *Journal of Manufacturing Processes*, vol. 36, pp. 571–600, Dec. 2018.

[2] A. P. Costa, L. Quintino, M. Greitmann, "Laser beam welding hard metals to steel," *Journal of Materials Processing Technology*, vol. 141, no. 2, pp. 163–173, Oct. 2003.

[3] L. K. Pan, C. C. Wang, Y. C. Hsiao, K. C. Ho, "Optimization of Nd:YAG laser welding onto magnesium alloy via Taguchi analysis," *Optics & Laser Technology*, vol. 37, no. 1, pp. 33–42, Feb. 2005.

[4] K. Y. Benyounis, A. G. Olabi, M. S. J. Hashmi, "Effect of laser welding parameters on the heat input and weld-bead profile," *Journal of Materials Processing Technology*, vol. 164–165, pp. 978–985, May 2005.

[5] A.-M. El-Batahgy, *Laser Beam Welding of Austenitic Stainless Steels – Similar Butt and Dissimilar Lap Joints*. 2012.

[6] D. Grevey, P. Sallamand, E. Cicala, S. Ignat, "Gas protection optimization during Nd:YAG laser welding," *Optics & Laser Technology*, vol. 37, no. 8, pp. 647–651, Nov. 2005.

[7] S. D. Sabdin, N. I. S. Hussein, M. K. Sued, M. S. Ayob, M. A. S. A. Rahim, M. Fadzil, "Effects of ColdArc welding parameters on the tensile strengths of high strength steel plate investigated using the Taguchi approach," *Journal of Mechanical Engineering and Sciences*, vol. 13, no. 2, pp. 4846–4856, 2019.

[8] J. R. Berretta, W. de Rossi, M. David Martins das Neves, I. Alves de Almeida, N. Dias Vieira Junior, "Pulsed Nd:YAG laser welding of AISI 304 to AISI 420 stainless steels," *Optics and Lasers in Engineering*, vol. 45, no. 9, pp. 960–966, Sep. 2007.

[9] K. Y. Benyounis, A. G. Olabi, M. S. J. Hashmi, "Multi-response optimization of CO2 laser-welding process of austenitic stainless steel," *Optics & Laser Technology*, vol. 40, no. 1, pp. 76–87, Feb. 2008.

[10] M. R. Nakhaei, N. B. Mostafa Arab, G. Naderi, "Application of response surface methodology for weld strength prediction in laser welding of polypropylene/clay nanocomposite," *Iranian Polymer Journal (English Edition)*, vol. 22, no. 5, pp. 351–360, 2013.

[11] S. Madhankumar, R. Balamurugan, S. Rajesh, "Investigations on austenitic nickel-chromium based super alloys - Inconel 625 and Inconel 718 from material removal rate in micro electrochemical machining," in *AIP conference Proceeding*, 2019, vol. 2128, p. 040009.

[12] S. Emami, T. Saeid, R. A. Khosroshahi, "Microstructural evolution of friction stir welded SAF 2205 duplex stainless steel," *Journal of Alloys and Compounds*, vol. 739, pp. 678–689, Mar. 2018.

[13] N. I. S. Hussein, S. Laily, M. S. Salleh, M. N. Ayof, "Statistical analysis of second repair welding on dissimilar material using Taguchi method," *Journal of Mechanical Engineering and Sciences*, vol. 13, no. 2, pp. 5021–5030, 2019.

[14] C. Li, J. Huang, K. Wang, Z. Chen, Q. Liu, "Optimization of processing parameters of laser skin welding in vitro combining the response surface methodology with NSGA- II," *Infrared Physics & Technology*, vol. 103, p. 103067, Dec. 2019.

[15] S. Bhavsar, P. Dudhagara, S. Tank, "R software package based statistical optimization of process components to simultaneously enhance the bacterial growth, laccase production and textile dye decolorization with cytotoxicity study," *PLoS One*, vol. 13, no. 5, pp. 1–18, 2018.

[16] S. K. Behera, H. Meena, S. Chakraborty, B. C. Meikap, "Application of response surface methodology (RSM) for optimization of leaching parameters for ash reduction from low-grade coal," *International Journal of Mining Science and Technology*, vol. 28, no. 4, pp. 621–629, Jul. 2018.

[17] I. Hanhan, R. Agyei, X. Xiao, M. D. Sangid, "Comparing non-destructive 3D X-ray computed tomography with destructive optical microscopy for microstructural characterization of fiber reinforced composites," *Composites Science and Technology*, vol. 184, p. 107843, Nov. 2019.

[18] A. Mortezaie and M. Shamanian, "An assessment of microstructure, mechanical properties and corrosion resistance of dissimilar welds between Inconel 718 and 310S austenitic stainless steel," *International Journal of Pressure Vessels and Piping.*, vol. 116, no. 1, pp. 37–46, 2014.

[19] G. N. Ahmad, M. S. Raza, N. K. Singh, and H. Kumar, "Experimental investigation on Ytterbium fiber laser butt welding of Inconel 625 and Duplex stainless steel 2205 thin sheets," *Optics & Laser Technology*, vol. 126, no. September 2019, p. 106117, 2020.

[20] S. Dev, K. D. Ramkumar, N. Arivazhagan, and R. Rajendran, "Investigations on the microstructure and mechanical properties of dissimilar welds of inconel 718 and sulphur rich martensitic stainless steel, AISI 416," *Journal of Manufacturing Processes*, vol. 32, no. March, pp. 685–698, 2018.

[21] W. Wang, Y. Lu, X. Ding, and T. Shoji, "Microstructures and microhardness at fusion boundary of 316 stainless steel/Inconel 182 dissimilar welding," *Materials Characterization*, vol. 107, pp. 255–261, 2015.

[22] Y. Zhang, H. Jing, L. Xu, Y. Han, L. Zhao, and B. Xiao, "Microstructure and mechanical performance of welded joint between a novel heat-resistant steel and Inconel 617 weld metal," *Materials Characterization* vol. 139, pp. 279–292, 2018.

[23] A. Kulkarni, D. K. Dwivedi, and M. Vasudevan, "Dissimilar metal welding of P91 steel-AISI 316L SS with Incoloy 800 and Inconel 600 interlayers by using activated TIG welding process and its effect on the microstructure and mechanical properties," *Journal of Materials Processing Technology*, vol. 274, no. July, p. 116280, 2019.